

# THE EFFECT OF THE HDDR PROCESS ON THE PRODUCTION OF Pr-Fe-Co-B-Nb SINTERED MAGNETS

**E. A. Ferreira, J. C. S. Casini, E. A. Périgo, R. N. Faria, H. Takiishi**

Av. Prof. Lineu Prestes, 2242 - CEP 05508-000, eaferreira@ipen.br

Instituto de Pesquisas Energéticas e Nucleares, IPEN-CNEN/SP, Brazil

## **ABSTRACT**

*Sintered magnets have been produced with powder obtained with the HDDR process. This new processing procedure for the production of the sintered magnets has been adopted in an attempt to reduce the milling time. Annealed ingot alloys based on the compositions  $Pr_{14}Fe_{75.9}Co_xB_6Nb_{0.1}$  ( $x = 0; 4; 8; 10; 12; 16$ ) have been employed in this investigation. A high rare earth content copper-containing alloy,  $Pr_{20.5}Fe_{bal}B_5Cu_{2.0}$ , was used as a sintering aid. A mixture of the HDDR powder obtained from these alloys was used to prepare sintered magnets. Standard hydrogen decrepitation (HD) magnets have also been included in this work for a comparison. A remanence of 1173 mT was achieved with the alloy  $Pr_{14}Fe_{67.9}Co_{16}B_6Nb_{0.1}$  processed using the HDDR process and a milling time of only 5 h. The microstructures of the magnets have been investigated by scanning electron microscopy and energy dispersive X-ray analysis.*

**Keywords:** Hydrogen Decrepitation, PrFeCoBNb magnets, HDDR Process

## **INTRODUCTION**

Currently, PrFeB-based sintered magnets with good magnetic properties have been produced using the hydrogen decrepitation process. The hydrogenation, disproportionation, desorption and recombination process, developed for Nakayama and Takeshita in 1989 [1], is a traditional method that become attractive in the production of magnetically coercive powders. Furthermore, HDDR magnets based on

praseodymium-iron-cobalt revealed to be much easier to prepare [2]. The influence of the milling time on the magnetic properties of sintered magnets has been studied in several works [3-5]. In this study, sintered HD magnets have been produced using a mixture of two alloys:  $\text{Pr}_{14}\text{Fe}_{\text{bal}}\text{Co}_x\text{B}_6\text{Nb}_{0.1}$  ( $x= 0; 4; 8; 10; 12; 16$ ) (80 wt.%) and  $\text{Pr}_{20.5}\text{Fe}_{72.5}\text{B}_5\text{Cu}_{2.0}$  (20 wt.%). These magnets have been prepared using conventional powder metallurgy and the HD process with a standard milling time of 20 hours. Using the same mixture of alloys the HDDR process was employed for production powders together a distinct processing route aiming the reduction of the milling time to 5 hours.

## MATERIALS AND METHODS

Several commercial  $\text{Pr}_{14}\text{Fe}_{\text{bal}}\text{Co}_x\text{B}_6\text{Nb}_{0.1}$  ( $x= 0; 4; 8; 10; 12; 16$ ) alloys in the annealed state (1070 °C for 20 h) were used in this investigation. No heat treatment was applied to the  $\text{Pr}_{20.5}\text{Fe}_{72.5}\text{B}_5\text{Cu}_{2.0}$  alloy employed as sintering aid. The final chemical composition of the magnets were  $\text{Pr}_{15.3}\text{Fe}_{\text{bal}}\text{Co}_x\text{B}_{5.8}\text{Nb}_{0.1}$  ( $x= 0; 2; 4; 5; 6; 8$ ). The study of the Co-containing alloys and the details of the preparation of the HD sintered magnets and HDDR magnets have already been described in previous papers [6,7]. The standard procedure (HD process) and the HDDR procedure used in this work for magnets production are the same procedures used in the reference [6] (standard procedure and route C process, respectively). The sintering step for all magnets was carried out at 1050°C for 1 hour. The processing temperatures (desorption/recombination) of HDDR process used for the improved magnetic properties for each alloy were: 820°C (0 and 10 at.% Co alloys), 840°C (4 at.% Co alloy) and 880°C (8, 12 and 16 at.% Co alloys) [7]. Magnetic measurements of the sintered magnets were performed in a permeameter after saturation in a pulsed field of 6 T. The squareness factor was determined from the demagnetization curve ( $\text{SF} = H_k/iH_c$ ). Magnet densities were measured using a liquid displacement system. The microstructures of the magnetic alloys were observed with a scanning electron microscope (SEM) and the phase compositions were determined with the aid of an energy dispersive X-ray (EDX) spectrometer system coupled to the SEM.

## RESULTS AND DISCUSSION

The variation in remanence and intrinsic coercivity of HD sintered magnets produced from a mixture of  $\text{Pr}_{14}\text{Fe}_{\text{bal}}\text{Co}_x\text{B}_6\text{Nb}_{0.1}$  ( $x= 0; 4; 8; 10; 12; 16$ ) (80 wt.%) and  $\text{Pr}_{20.5}\text{Fe}_{72.5}\text{B}_5\text{Cu}_{2.0}$  (20 wt.%) alloys as a function of cobalt content is shown in Figure 1. The best remanence was observed with  $\text{Pr}_{14}\text{Fe}_{75.9}\text{Co}_4\text{B}_6\text{Nb}_{0.1}$  alloy (1220 mT). The HD sintered magnet produced with  $\text{Pr}_{14}\text{Fe}_{67.9}\text{Co}_{12}\text{B}_6\text{Nb}_{0.1}$  alloy also showed good remanence (1210 mT). The highest intrinsic coercivity (952 kA/m) was achieved in the sample prepared using the alloy with 4 at% cobalt.

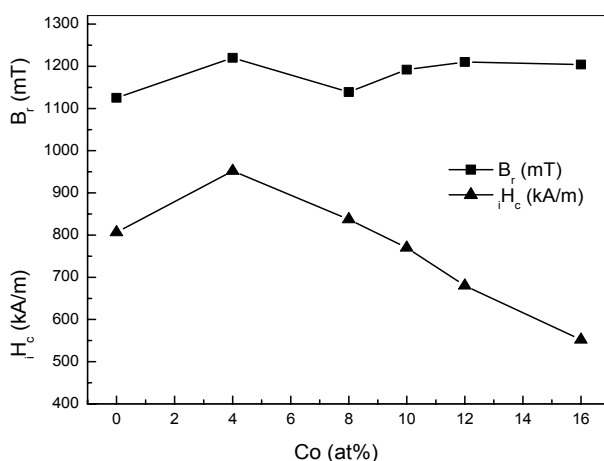


**Figure 1** - Remanence and intrinsic coercivity versus cobalt content for HD sintered permanent magnets produced with  $\text{Pr}_{14}\text{Fe}_{\text{bal}}\text{Co}_x\text{B}_6\text{Nb}_{0.1}$  ( $x= 0; 4; 8; 10; 12; 16$ ) alloys.

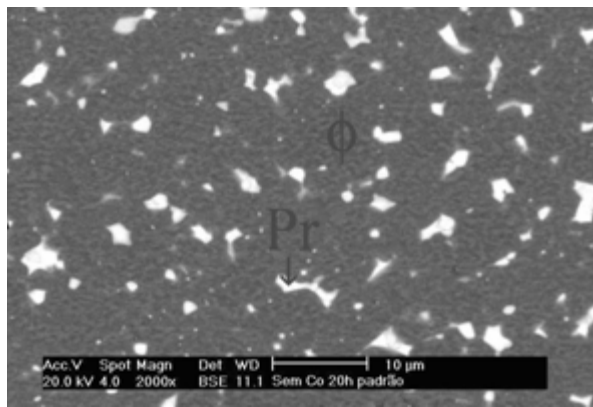
A summary of the magnetic properties and density of the HD magnets prepared with  $\text{Pr}_{14}\text{Fe}_{\text{bal}}\text{Co}_x\text{B}_6\text{Nb}_{0.1}$  ( $x= 0; 4; 8; 10; 12; 16$ ) alloys is given in Table 1. The magnet produced with  $\text{Pr}_{14}\text{Fe}_{67.9}\text{Co}_{12}\text{B}_6\text{Nb}_{0.1}$  alloy exhibited the best remanence and density ( $7.41 \text{ g/cm}^3$ ). A satisfactory density for this kind of magnets stays between  $7.0$  and  $7.5 \text{ g/cm}^3$ , or 92 to 99% of the theoretical density [8]. The highest energy product ( $283 \text{ kJ/m}^3$ ) was exhibited by the magnet produced with  $\text{Pr}_{14}\text{Fe}_{63.9}\text{Co}_4\text{B}_6\text{Nb}_{0.1}$  alloy, together with the best squareness factor ( $\text{SF}=0.88$ ).

**Table 1** - Magnetic properties and density of the HD magnets prepared with  $\text{Pr}_{14}\text{Fe}_{\text{bal}}\text{Co}_x\text{B}_6\text{Nb}_{0.1}$  ( $x= 0; 4; 8; 10; 12; 16$ ) alloys (error:  $\pm 2\%$ ).

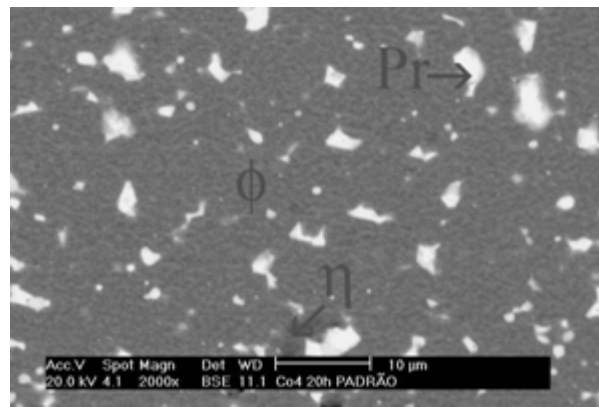
HD Process (20 h)	$B_r$ (mT)	$iH_c$ (kA/m)	$bH_c$ (kA/m)	$(BH)_{\text{máx}}$ (kJ/m <sup>3</sup> )	SF (ratio)	$\rho$ (g/cm <sup>3</sup> )
$\text{Pr}_{14}\text{Fe}_{79.9}\text{B}_6\text{Nb}_{0.1}$	1125	806	706	224	0.85	7.19
$\text{Pr}_{14}\text{Fe}_{75.9}\text{Co}_4\text{B}_6\text{Nb}_{0.1}$	1220	952	880	283	0.88	7.38
$\text{Pr}_{14}\text{Fe}_{71.9}\text{Co}_8\text{B}_6\text{Nb}_{0.1}$	1139	837	672	236	0.83	7.07
$\text{Pr}_{14}\text{Fe}_{69.9}\text{Co}_{10}\text{B}_6\text{Nb}_{0.1}$	1192	770	647	245	0.81	7.27
$\text{Pr}_{14}\text{Fe}_{67.9}\text{Co}_{12}\text{B}_6\text{Nb}_{0.1}$	1210	680	584	239	0.82	7.41
$\text{Pr}_{14}\text{Fe}_{63.9}\text{Co}_{16}\text{B}_6\text{Nb}_{0.1}$	1204	552	424	249	0.85	7.33

The microstructures of the HD magnets prepared from the  $\text{Pr}_{14}\text{Fe}_{\text{bal}}\text{Co}_x\text{B}_6\text{Nb}_{0.1}$  alloys are shown in Fig. 2 (a-f). Five phases were identified: the matrix phase ( $\phi$ ), Pr rich phases  $\text{Pr}_3(\text{FeCo})$  and  $\text{Pr}_2(\text{FeCo})$  in the grain boundaries of the matrix phase, boron rich phase  $\text{Pr}_{1+\epsilon}\text{Fe}_4\text{B}_4$  ( $\eta$ ) and the Laves Phase  $\text{Pr}(\text{FeCo})_2$  (phases are labeled in the micrographics). The boron rich phase  $\text{Pr}_{1+\epsilon}\text{Fe}_4\text{B}_4$  ( $\eta$ ) was identified by the Fe:Pr ratio [9]. The Laves phase was found in magnets produced using 10, 12 and 16 at.%Co. The  $\text{Pr}_2(\text{FeCo})$  phase was found only in the magnet produced using 8 at.% Co.

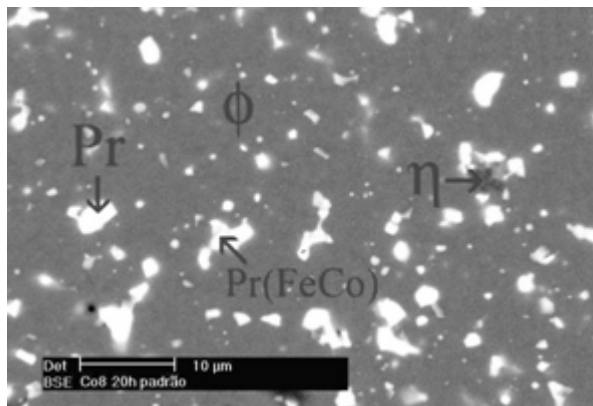
It has been reported that the Laves phase  $\text{Pr}(\text{FeCo})_2$  is detrimental to the intrinsic coercivity of rare earth-based sintered magnets [10]. This phase can be detected in the grain boundary of matrix phase together with the Pr-rich phase and was not found in the magnets with low levels of cobalt (see Figs. 2 a-c). The chemical compositions of the phases determined by EDX for HD magnets obtained with  $\text{Pr}_{14}\text{Fe}_{\text{bal}}\text{Co}_x\text{B}_6\text{Nb}_{0.1}$  ( $x= 0; 4; 8; 10; 12; 16$ ) alloys are given in Table 2.



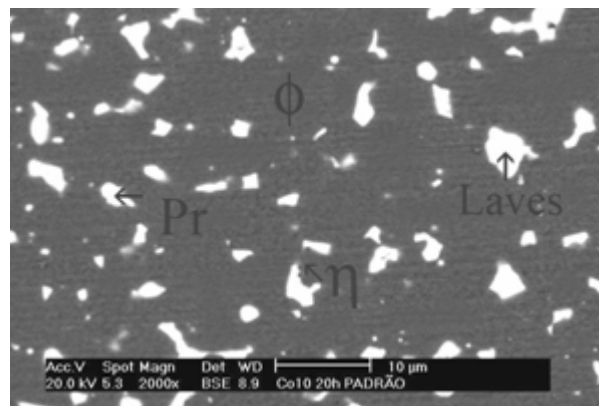
(a)



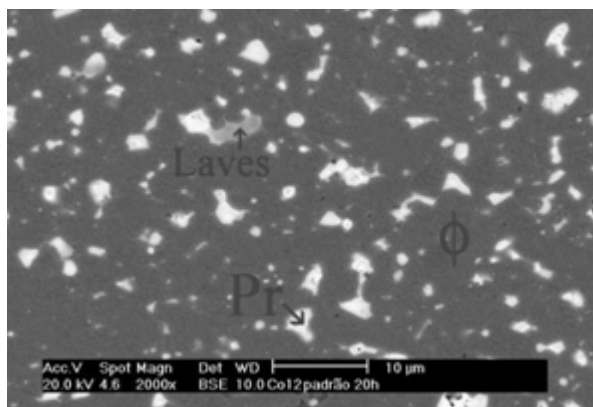
(b)



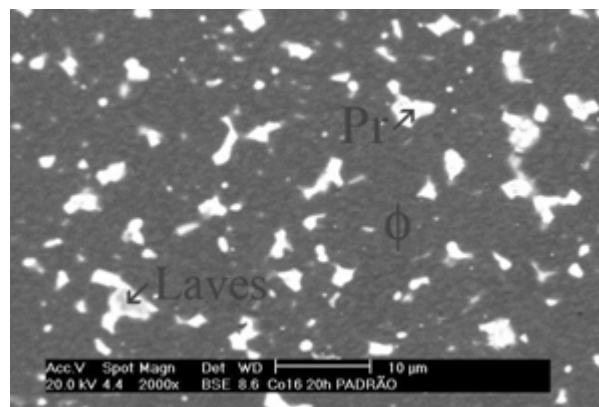
(c)



(d)



(e)



(f)

**Figure 2** - Microstructures of the Pr-based HD magnets based on the compositions: (a)  $\text{Pr}_{14}\text{Fe}_{79.9}\text{B}_6\text{Nb}_{0.1}$ , (b)  $\text{Pr}_{14}\text{Fe}_{75.9}\text{B}_6\text{Co}_4\text{Nb}_{0.1}$ , (c)  $\text{Pr}_{14}\text{Fe}_{71.9}\text{B}_6\text{Co}_8\text{Nb}_{0.1}$ , (d)  $\text{Pr}_{14}\text{Fe}_{69.9}\text{B}_6\text{Co}_{10}\text{Nb}_{0.1}$ , (e)  $\text{Pr}_{14}\text{Fe}_{67.9}\text{B}_6\text{Co}_{12}\text{Nb}_{0.1}$  and (f)  $\text{Pr}_{14}\text{Fe}_{63.9}\text{B}_6\text{Co}_{16}\text{Nb}_{0.1}$  (2000x).

**Table 2** - Chemical composition determined by EDX for the phases found in the HD magnets prepared with  $\text{Pr}_{14}\text{Fe}_{\text{bal}}\text{Co}_x\text{B}_6\text{Nb}_{0.1}$  alloys (error:  $\pm 2\%$ ).

HD Process	Phase	Pr (% at.)	Fe (% at.)	Co (% at.)	Pr:(Fe;Co) ratio
<b>0 at.%Co</b>	$\text{Pr}_2\text{Fe}_{14}\text{B}$ ( $\phi$ )	14.19	85.81	-	2 : (12.1)
	$\text{Pr}_3\text{Fe}$ (Pr rico)	75.43	24.57	-	3: (1)
<b>4 at.%Co</b>	$\text{Pr}_2(\text{FeCo})_{14}\text{B}$ ( $\phi$ )	13.83	82.26	3.91	2:(11.9;0.6)
	$\text{Pr}_3(\text{FeCo})$ (Pr rich)	80.57	17.64	1.79	3:(0.7;0.1)
	$\text{Pr}_{1+\varepsilon}(\text{FeCo})_4\text{B}_4$ ( $\eta$ )	29.36	54.68	15.96	1:(1.8;0.5)
<b>8 at.%Co</b>	$\text{Pr}_2(\text{FeCo})_{14}\text{B}$ ( $\phi$ )	13.28	76.05	10.67	2:(11.5;1.61)
	$\text{Pr}_3(\text{FeCo})$ (Pr rich)	73.41	22.66	3.93	3:( 0.93;0.16)
	$\text{Pr}_2(\text{FeCo})$ (Pr rich)	60.84	33.58	5.58	2:( 1,10; 0.18)
	$\text{Pr}_{1+\varepsilon}(\text{FeCo})_4\text{B}_4$ ( $\eta$ )	28.43	57.62	13.95	1: (2.03; 0.49)
<b>10 at.%Co</b>	$\text{Pr}_2(\text{FeCo})_{14}\text{B}$ ( $\phi$ )	14.12	75.87	10.01	2:(10.75;1.41)
	$\text{Pr}_3(\text{FeCo})$ (Pr rich)	73.49	20.96	5.55	3:(0.85;0.23)
	$\text{Pr}(\text{FeCo})_2$ (Laves)	34.86	29.67	35.47	1:(0.85;1.02)
	$\text{Pr}_{1+\varepsilon}(\text{FeCo})_4\text{B}_4$ ( $\eta$ )	26.59	57.38	16.03	1:(2.16;0.60)
<b>12 at.%Co</b>	$\text{Pr}_2(\text{FeCo})_{14}\text{B}$ ( $\phi$ )	13.93	76.84	9.23	2:(11.03;1.32)
	$\text{Pr}_3(\text{FeCo})$ (Pr rich)	74.67	21.45	3.88	3:(0.86;0.15)
	$\text{Pr}(\text{FeCo})_2$ (Laves)	29.46	35.52	35.02	1:(1.20;1.18)
<b>16 at.%Co</b>	$\text{Pr}_2(\text{FeCo})_{14}\text{B}$ ( $\phi$ )	12.91	74.94	12.15	2:(11.61;1.88)
	$\text{Pr}_3(\text{FeCo})$ (Pr rich)	75.52	21.83	2.65	3:(0.86;0.10)
	$\text{Pr}(\text{FeCo})_2$ (Laves)	32.71	33.27	34.02	1:(1.05;1.04)

The variation in remanence and intrinsic coercivity of HDDR sintered magnets produced from a mixture of Pr-based alloys as a function of cobalt content is shown in Figure 3. The best remanence was observed for the HDDR sintered magnet produced with  $\text{Pr}_{14}\text{Fe}_{63.9}\text{B}_6\text{Co}_{16}\text{Nb}_{0.1}$  alloy (1173 mT) but with a rather low intrinsic coercivity (518 kA/m). The highest intrinsic coercivity (816 kA/m) was achieved in the HDDR sintered magnet produced with the  $\text{Pr}_{14}\text{Fe}_{75.9}\text{B}_6\text{Co}_4\text{Nb}_{0.1}$  alloy.

A summary of the magnetic properties and density the HDDR magnets are shown in Table 3. It is worth noting that cobalt addition in the magnetic alloy increased the remanence in the HD sintered magnets from 1057 to 1173 mT. In contrast, the intrinsic coercivity decreased considerably in the magnet with 16 at.% of this element. The highest energy product ( $241 \text{ kJ/m}^3$ ) was exhibited by the HDDR magnet produced with the  $\text{Pr}_{14}\text{Fe}_{75.9}\text{B}_6\text{Co}_4\text{Nb}_{0.1}$  alloy, which also showed the best squareness factor

(SF=0.83). The HDDR process decreased slightly the magnetic properties, but, on the other hand, reduced in 75% the milling time.

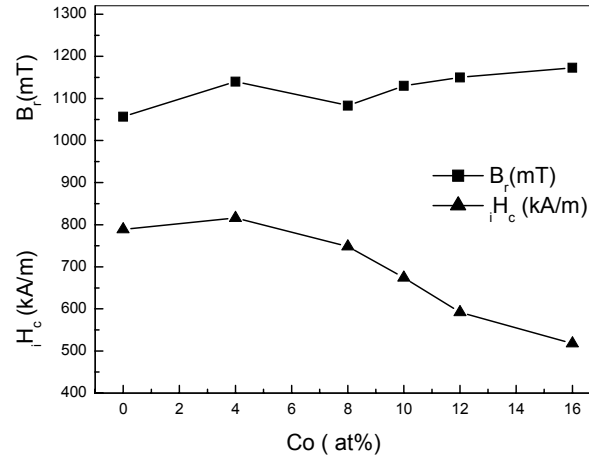


**Figure 3** - Remanence and intrinsic coercivity versus cobalt content for HDDR sintered permanent magnets produced with  $\text{Pr}_{14}\text{Fe}_{\text{bal}}\text{Co}_x\text{B}_6\text{Nb}_{0.1}$  ( $x=0; 4; 8; 10; 12; 16$ ) alloys.

**Table 3** - Magnetic properties and density of the HDDR magnets prepared with  $\text{Pr}_{14}\text{Fe}_{\text{bal}}\text{Co}_x\text{B}_6\text{Nb}_{0.1}$  ( $x=0; 4; 8; 10; 12; 16$ ) alloys (error:  $\pm 3\%$ ).

HDDR Process (5 h)	$B_r$ (mT)	$iH_c$ (kA/m)	$bH_c$ (kA/m)	$(BH)_{\text{máx}}$ (kJ/m <sup>3</sup> )	SF (ratio)	$\rho$ (g/cm <sup>3</sup> )
$\text{Pr}_{14}\text{Fe}_{79.9}\text{B}_6\text{Nb}_{0.1}$	1057	789	663	206	0.78	7.05
$\text{Pr}_{14}\text{Fe}_{75.9}\text{Co}_4\text{B}_6\text{Nb}_{0.1}$	1140	816	648	241	0.83	7.31
$\text{Pr}_{14}\text{Fe}_{71.9}\text{Co}_8\text{B}_6\text{Nb}_{0.1}$	1083	748	624	221	0.81	7.35
$\text{Pr}_{14}\text{Fe}_{69.9}\text{Co}_{10}\text{B}_6\text{Nb}_{0.1}$	1130	674	552	230	0.80	7.26
$\text{Pr}_{14}\text{Fe}_{67.9}\text{Co}_{12}\text{B}_6\text{Nb}_{0.1}$	1150	592	504	228	0.75	7.34
$\text{Pr}_{14}\text{Fe}_{63.9}\text{Co}_{16}\text{B}_6\text{Nb}_{0.1}$	1173	518	410	224	0.77	7.22

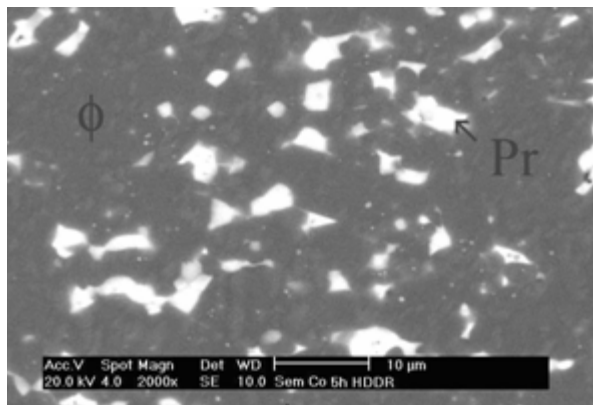
The microstructures of the HDDR magnets obtained with the  $\text{Pr}_{14}\text{Fe}_{\text{bal}}\text{Co}_x\text{B}_6\text{Nb}_{0.1}$  ( $x= 0; 4; 8; 10; 12; 16$ ) alloys are shown in Figs. 4 (a-f). The phases found in the HDDR magnets are the same five phases identified in the HD magnets.

The intrinsic coercivity decreased with the addition of cobalt in the HD and HDDR permanent magnets due to the presence of a  $\text{Pr}(\text{FeCo})_2$  phase. This phase has also been identified in a previous work [10]. The chemical compositions of the phases determined by EDX for HDDR magnets obtained with  $\text{Pr}_{14}\text{Fe}_{\text{bal}}\text{Co}_x\text{B}_6\text{Nb}_{0.1}$  ( $x= 0; 4; 8; 10; 12; 16$ ) alloys are given in Table 4.

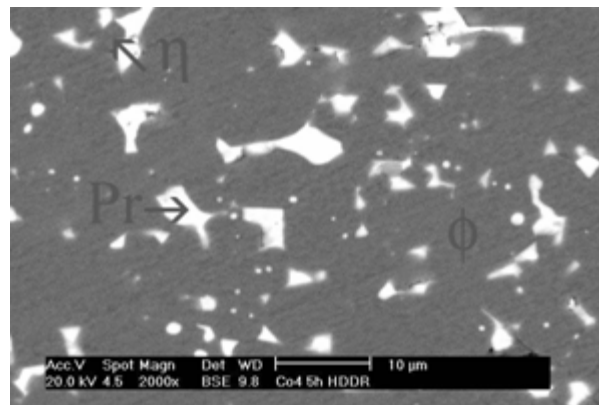
**Table 4** - Chemical composition determined by EDX for the phases present on the HDDR magnets prepared with the  $\text{Pr}_{14}\text{Fe}_{\text{bal}}\text{Co}_x\text{B}_6\text{Nb}_{0.1}$  alloys (error:  $\pm 2\%$ ).

HDDR Process	Phases	Pr (% at.)	Fe (% at.)	Co (% at.)	Pr:(Fe;Co) ratio
0 at.%Co	$\text{Pr}_2\text{Fe}_{14}\text{B}$ ( $\phi$ )	13.75	86.25	-	2:(12.54)
	$\text{Pr}_3\text{Fe}$ (Pr rico)	73.29	26.71	-	3:(1.09)
4 at.%Co	$\text{Pr}_2(\text{FeCo})_{14}\text{B}$ ( $\phi$ )	13.58	81.67	4.75	2:(12.02;0.70)
	$\text{Pr}_3(\text{FeCo})$ (Pr rich)	80.53	17.41	2.06	3:(0.64;0.07)
	$\text{Pr}_{1+\epsilon}(\text{FeCo})_4\text{B}_4$ ( $\eta$ )	30.88	53.17	15.95	1:(1.72;0.51)
8 at.%Co	$\text{Pr}_2(\text{FeCo})_{14}\text{B}$ ( $\phi$ )	13.97	76.11	9.92	2:(10.89;1.42)
	$\text{Pr}_3(\text{FeCo})$ (Pr rich)	75.06	21.68	3.26	3:(0.86;0.13)
	$\text{Pr}_2(\text{FeCo})$ (Pr rich)	58.97	35.70	5.33	2:(1,21;0.18)
	$\text{Pr}_{1+\epsilon}(\text{FeCo})_4\text{B}_4$ ( $\eta$ )	29.14	58.95	11.91	1:(2.02;0.40)
10 at.%Co	$\text{Pr}_2(\text{FeCo})_{14}\text{B}$ ( $\phi$ )	14.15	76.30	9.55	2:(10.78;1.35)
	$\text{Pr}_3(\text{FeCo})$ (Pr rich)	75.02	21.39	3.59	3: (0.85;0.14)
	$\text{Pr}(\text{FeCo})_2$ (Laves)	31.99	30.67	37.34	1:(0.95;1.16)
	$\text{Pr}_{1+\epsilon}(\text{FeCo})_4\text{B}_4$ ( $\eta$ )	30.79	56.92	12.29	1:(1.84;0.40)
12 at.%Co	$\text{Pr}_2(\text{FeCo})_{14}\text{B}$ ( $\phi$ )	14.04	76.62	9.34	2:(10.91;1.33)
	$\text{Pr}_3(\text{FeCo})$ (Pr rich)	74.76	21.42	3.82	3:(0.86;0.15)
	$\text{Pr}(\text{FeCo})_2$ (Laves)	32.44	35.53	32.03	1:(1.08;0.98)
16 at.%Co	$\text{Pr}_2(\text{FeCo})_{14}\text{B}$ ( $\phi$ )	15.23	76.04	8.73	2:(9.98;1.14)
	$\text{Pr}_3(\text{FeCo})$ (Pr rich)	74.33	21.74	3.93	3:(0.87;0.16)
	$\text{Pr}(\text{FeCo})_2$ (Laves)	33.36	34.91	31.73	1:(1.05;0.95)

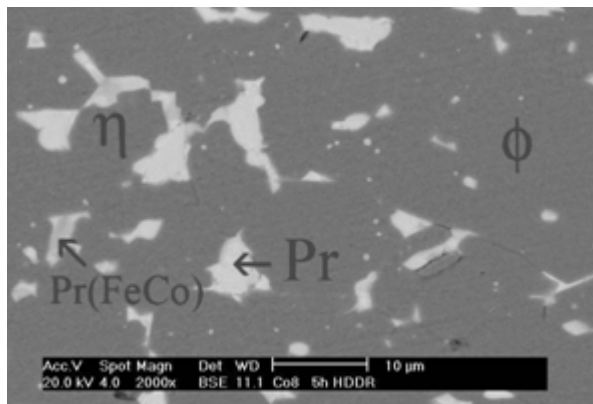




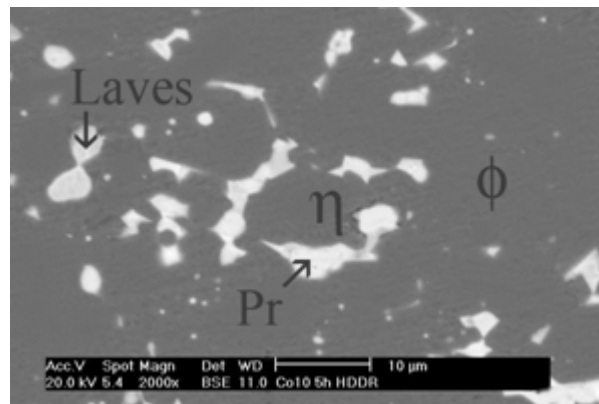
(a)



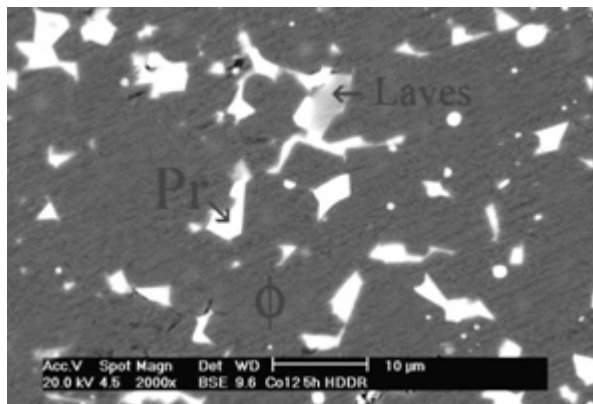
(b)



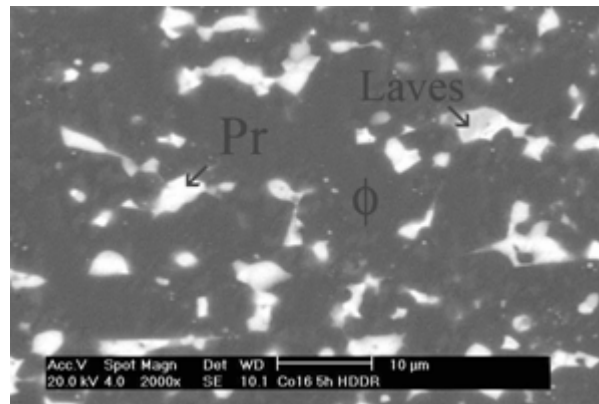
(c)



(d)



(e)



(f)

**Figure 4** - Microstructures of the Pr-based HDDR magnets based on the compositions: (a)  $\text{Pr}_{14}\text{Fe}_{79.9}\text{B}_6\text{Nb}_{0.1}$  , (b)  $\text{Pr}_{14}\text{Fe}_{75.9}\text{Co}_4\text{B}_6\text{Nb}_{0.1}$  , (c)  $\text{Pr}_{14}\text{Fe}_{71.9}\text{Co}_8\text{B}_6\text{Nb}_{0.1}$ , (d)  $\text{Pr}_{14}\text{Fe}_{69.9}\text{Co}_{10}\text{B}_6\text{Nb}_{0.1}$ , (e)  $\text{Pr}_{14}\text{Fe}_{67.9}\text{Co}_{12}\text{B}_6\text{Nb}_{0.1}$  and (f)  $\text{Pr}_{14}\text{Fe}_{63.9}\text{Co}_{16}\text{B}_6\text{Nb}_{0.1}$  (2000x).

Fig 5 (a-d) shows the change in the grain size of the HD and HDDR magnets produced with alloys containing 8 and 16 at.% Co. The grain size of the matrix phase in the magnets HD and HDDR increased with higher Co content.

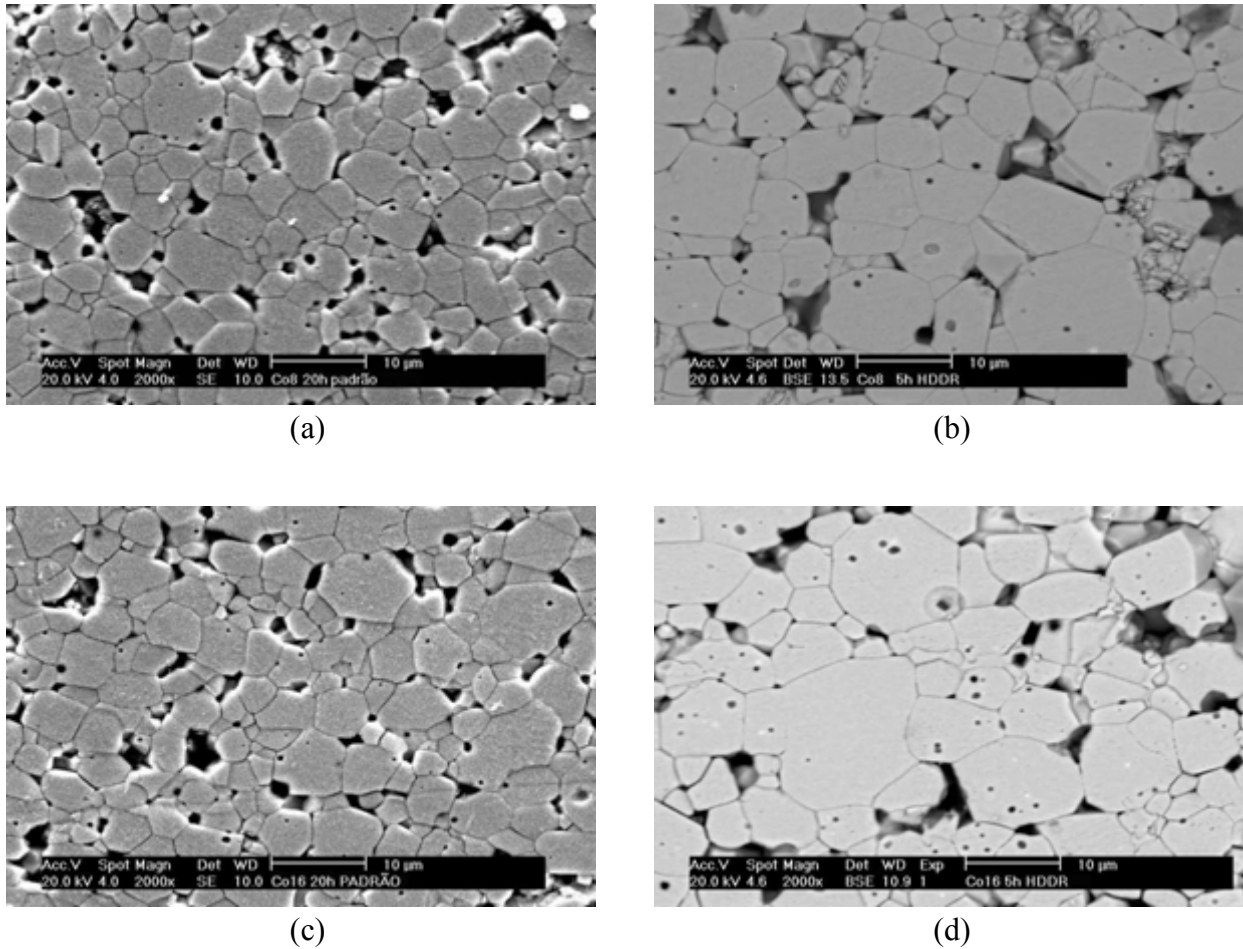


**Figure 5** - Evolution of the grain size in the magnets obtained with  $\text{Pr}_{14}\text{Fe}_{\text{bal}}\text{Co}_x\text{B}_6\text{Nb}_{0.1}$  ( $x= 8;16$ ) alloys : (a)  $\text{Co}_8$  – HD process, (b)  $\text{Co}_8$  - HDDR process , (c)  $\text{Co}_{16}$  – HD process, (d)  $\text{Co}_{16}$  - HDDR process, (2000x).

The grain size and standard deviation in the HD and HDDR sintered magnets obtained with the  $\text{Pr}_{14}\text{Fe}_{\text{bal}}\text{Co}_x\text{B}_6\text{Nb}_{0.1}$  ( $x= 0; 4; 8; 10; 12; 16$ ) alloys are given in Table 5. The magnetic properties decreased on the HDDR magnets due to the abnormal increase in the grain size and reduced magnetic isolation of the matrix phase.

**Table 5** - Grain size and standard deviation in the HD and HDDR sintered magnets obtained with  $\text{Pr}_{14}\text{Fe}_{\text{bal}}\text{Co}_x\text{B}_6\text{Nb}_{0.1}$  ( $x= 0; 4; 8; 10; 12; 16$ ) alloys (error:  $\pm 3\%$ ).

Alloy used in the magnet's production	HD Process		HDDR Process	
	Grain size ( $\mu\text{m}$ )	Standard deviation	Grain size ( $\mu\text{m}$ )	Standard deviation
$\text{Pr}_{14}\text{Fe}_{79.9}\text{B}_6\text{Nb}_{0.1}$	3.03	2.11	5.51	2.12
$\text{Pr}_{14}\text{Fe}_{75.9}\text{Co}_4\text{B}_6\text{Nb}_{0.1}$	3.04	2.04	5.46	1.97
$\text{Pr}_{14}\text{Fe}_{71.9}\text{Co}_8\text{B}_6\text{Nb}_{0.1}$	3.11	2.15	5.43	2.21
$\text{Pr}_{14}\text{Fe}_{69.9}\text{Co}_{10}\text{B}_6\text{Nb}_{0.1}$	3.06	2.01	5.59	2.04
$\text{Pr}_{14}\text{Fe}_{67.9}\text{Co}_{12}\text{B}_6\text{Nb}_{0.1}$	3.10	1.90	5.58	2.07
$\text{Pr}_{14}\text{Fe}_{63.9}\text{Co}_{16}\text{B}_6\text{Nb}_{0.1}$	3.02	1.94	5.53	2.19

## CONCLUSIONS

The HDDR process can be included in the production of sintered Pr-based magnets in order to reduce the milling time. A particular HDDR route was required to reduce the processing time, but at the expenses of the magnetic properties. The presence of Laves phase in the Pr-Fe-Co-B-Nb magnets produced by HD and HDDR process with 10 at%, 12 at% and 16 at% Co was detrimental to the intrinsic coercivity. The HD process promoted some grain size refinement of the hard magnetic matrix phase, good magnetic isolation and, hence, an increase in  $iH_c$ . Conversely, the introduction of the HDDR process led to a reduction in the isolation of the magnetic grains and somewhat inferior magnetic properties.

## ACKNOWLEDGMENTS

Many thanks are due to FAPESP, CNPQ and IPEN-CNEN/SP for supporting this investigation.

## REFERENCES

- [1] Takeshita, T. and Nakayama, R. : **10<sup>th</sup> Int. Workshop on RE Magnets and Their Applications**, Kyoto, p. 551-557, 1989.
- [2] Faria, R.N. ; Williams, A.J. and Harris, I.R. : **Journal of Alloys and Compounds**, v.287, p.10-12, 1999.
- [3] Noh, T.H. ; Jeung, W.Y. ; Kang, I.K. ; Shin, S. H. and Lee,J. J. : **Journal of Applied Physics**, v. 70, n. 10, p. 6591-6593, 1991.
- [4] Faria, R.N. ; Abell, J. S. and Harris, I.R. : **Journal of Alloys and Compounds**, v. 177, p. 311-320, 1991.
- [5] Faria, R.N. ; Williams, A.J. ; Abell, J. S. and Harris, I.R. : **14<sup>th</sup> Int. Workshop on RE Magnets And Their Applications**, September 1-4, 1996, São Paulo, Brazil, p. 570-579.
- [6] Ferreira, E.A. ; Silva, S.C. ; Périgo, E.A. ; Faria, R.N. and Takiishi,H. : **Materials Science Forum**, v. 591-593, p. 885-890, 2008.
- [7] Silva, S.C. ; Ferreira, E.A. ; Faria, R.N. and Takiishi,H. : **Materials Science Forum**, v. 591-593, p. 108-113, 2008.
- [8] Jinghua, T. ; Yiying, H. ; Jingkui, L. T. : **Scientia Sinica**, vol.XXX, n. 6, p 607-619, 1987.
- [9] Faria, R.N. ; Takiishi,H. ; Castro, A. R. M. ; Lima, L. F. C. P. and Costa I. : **Journal of Magnetism and Magnetic Materials**, v. 246, p. 351-359, 2002.
- [10] Kim, A.S. : **Journal of Applied Physics**, v.63, n. 8, p. 3975, 1988